PROCEEDINGS OF SCIENCE

Faddeev Calculation of Hypertriton Including with YNN Three-Body Force

Hiroyuki Kamada,[a,b,*] **Michio Kohno**[b] **and Kazuya Miyagawa**[b]

[a] *Department of Physics, Faculty of Engineering, Kyushu Institution of Technology, 1-1 Sensuicho Tobata, Kitakyushu 804-8550, Japan*

[b] *Research Center for Nuclear Physics, Osaka University, 10-1 Mihogaoka, Ibaraki, Osaka 567-0047, Japan*

E-mail: kamada@rcnp.osaka-u.ac.jp, kohno@rcnp.osaka-u.ac.jp, miyagawa@rcnp.osaka-u.ac.jp

Calculations have been performed for the Faddeev three-body equations of Hypertriton using the SMS chiral potential for NN interactions, the Jülich-Bonn NLO19 chiral potential for YN interactions, and the YNN three-body force as inputs. For the YNN three-body force, not only a 2π exchange type but also 1π exchange and contact types were adopted. Partial wave expansion was performed to examine the effects of each type. It is understood that in chiral NLO order, it is not possible to determine the low-energy coefficients (LECs) of the three-body force. However, the range dependence of the high momentum cutoff is examined.

The 11th International Workshop on Chiral Dynamics (CD2024)
26–30 August 2024
Ruhr University Bochum, Germany

*Speaker

 ISSN 1824-8039 . Published by SISSA Medialab.

PoS(CD2024)094

1. introduction

The hypertriton is an exotic atomic nucleus consisting of a proton, a neutron, and a Λ particle. Nucleon-nucleon (NN) interactions have long been theoretically described using phenomenological potentials based on the meson theory. However, the precision in identifying the parameters included in the potential for the interaction between hyperon and nucleon (YN) is poor due to the short lifetime of the Λ particle and the lack of experimental data. On the other hand, three-body systems can be accurately described by using the Faddeev equations. We have carried out ab initio calculations to directly solve the Faddeev equations using conventional meson-theoretic potentials[1]. The meson-theoretical potential employed was that of the Nijmegen group for both NN[2] and YN[3]. Using the wave function of the hypertriton obtained by the calculation, we have been obtaining the decay rate and the lifetime of the hypertriton in weak decay[4]. Fortunately, a recent experimental paper (ALICE) [5] has indicated that our theoretical values are in closest agreement with the measured values.

Departing from the conventional meson theory, the chiral effective field theory [6] was proposed. This theory is an extension of the so-called Weinberg model, and it considers the Lagrangian interaction terms between nucleons and pions from the perspective of chiral symmetry. Subsequently, a potential [7] between nucleons was constructed based on this theory. In line with this chiral effective field theory, Jülich-Bonn's group proposed a potential between the hyperon and the nucleon, and research has been conducted on few-body systems including hyperons [8, 9]. Furthermore, it is now possible to calculate the three-body forces (3BF) derived from the Lagrangian of the chiral effective field theory[10]. In recent years, we have programmed the three-body force, especially the 2π exchange type [11]. Using the NN and YN potentials of the chiral effective field theory, we have performed a pioneering calculation of the Hypertriton including the 3BF of the 2π exchange type [12]. After that, calculations were carried out including not only the 2π exchange type but also 1π exchange type and contact type 3BFs [13]. In the course of conducting benchmark tests [14] on three-body forces in collaboration with Jülich-Bonn's group, a bug was identified in our three-body force code. Consequently, we undertook a reversion of three papers[11–13].[1]

In this workshop talk, the resulting wave functions are investigated. In the subsequent section, a brief introduction is provided to these 3BFs. In Section 3, we provide a more detailed discussion of the binding energy of hypertriton presented in our recent papers [12, 13]. In order to investigate the properties of the wave functions, a comparison of the expectation value of the kinetic energy with various potentials is made in Section 4. Our conclusion and outlook are presented in Section 5.

2. YNN three-body forces

As published in [10][12][13], the basic three-body force can be classified into three types: 2π exchange type, 1π exchange type, and contact type. This classification depends on the NNLO order

[1] Please note that Erratum is included in the references[11–13].

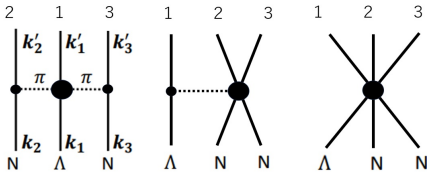

Figure 1: Diagram of 2π exchange, 1 π exchange and contact types ΛNN 3BF. For 2π exchange 3BF, the small filled circle denotes the NNπ vertex with the coupling constant g_A/f_0^2, and the large filled circle represents the NN$\pi\pi$ vertex specified by the coupling constants $3b_0 + b_D$ and $2b_2 + 3b_4$ in Eq. (1) of Ref. [11]. For 1 π exchange 3BF, the small filled circle denotes the NNπ vertex with the coupling constant g_A/f_0^2 again, and the large filled circle represents the NNNNπ vertex specified by the coupling constants in Eq. (2). And for the contact π exchange 3BF, the large filled circle represents $\Lambda\Lambda$NNNN coupling by the coupling constants in Eq. (3).

of chiral perturbation theory. The equations for these three-body forces are listed below in the order of 2π exchange type (2π), 1π exchange type (1π), and contact type (cont.);

$$\underline{2\pi \text{ exchange term}}: \quad V_{2\pi}^{\Lambda\text{NN}} = \frac{g_A^2}{3f_0^4}(\boldsymbol{\tau}_2\cdot\boldsymbol{\tau}_3)\frac{(\boldsymbol{\sigma}_3\cdot\boldsymbol{q}_{3d})(\boldsymbol{\sigma}_2\cdot\boldsymbol{q}_{2d})}{(\boldsymbol{q}_{3d}^2+m_\pi^2)(\boldsymbol{q}_{2d}^2+m_\pi^2)} \times\{-(3b_0+b_D)m_\pi^2+(2b_2+3b_4)\boldsymbol{q}_{3d}\cdot\boldsymbol{q}_{2d}\}, \tag{1}$$

where $\boldsymbol{q}_{2d}$ ($\boldsymbol{q}_{3d}$) is the difference between the final and initial momenta at the nucleon line 2 (line 3) of figure 1: $\boldsymbol{q}_{2d} = \boldsymbol{k}'_2 - \boldsymbol{k}_2$ and $\boldsymbol{q}_{3d} = \boldsymbol{k}'_3 - \boldsymbol{k}_3$, and $\boldsymbol{k}_i$ are free momentum of the i-th particle. g_A is the axial coupling constant, f_0 is the pion decay constant, m_π is the pion mass, and $\boldsymbol{\sigma}_i$ and $\boldsymbol{\tau}_i$ stand for the spin and isospin operators of the nucleon i (with $i = 2, 3$), respectively. The coupling constants b_0, b_D, b_2, and b_4 are those in the underlying $\Lambda\Lambda\pi\pi$ Lagrangian. These coupling constants are to be determined in parametrizing ΛN interactions in the next-to-next-to-leading order.

$$\underline{1\pi \text{ exchange term}}: \quad V_{1\pi}^{\Lambda NN} = -\frac{g_A}{2f_0^2}(\boldsymbol{\tau}_2\cdot\boldsymbol{\tau}_3) \times\left\{\frac{\boldsymbol{\sigma}_2\cdot\boldsymbol{q}_{2d}}{\boldsymbol{q}_{2d}^2+m_\pi^2}(D'_1\boldsymbol{\sigma}_1+D'_2\boldsymbol{\sigma}_3)\cdot\boldsymbol{q}_{2d} +\frac{\boldsymbol{\sigma}_3\cdot\boldsymbol{q}_{3d}}{\boldsymbol{q}_{3d}^2+m_\pi^2}(D'_1\boldsymbol{\sigma}_1+D'_2\boldsymbol{\sigma}_2)\cdot\boldsymbol{q}_{3d}\right\}, \tag{2}$$

and

$$\underline{\text{contact term}}: \quad V_{\text{cont}}^{\Lambda NN} = C'_1(1-\boldsymbol{\sigma}_2\cdot\boldsymbol{\sigma}_3)(3+\boldsymbol{\tau}_2\cdot\boldsymbol{\tau}_3) + C'_2(\boldsymbol{\sigma}_\Lambda\cdot(\boldsymbol{\sigma}_2+\boldsymbol{\sigma}_3))(1-\boldsymbol{\tau}_2\cdot\boldsymbol{\tau}_3) + C'_3(3+\boldsymbol{\sigma}_2\cdot\boldsymbol{\sigma}_3)(1-\boldsymbol{\tau}_2\cdot\boldsymbol{\tau}_3). \tag{3}$$

These three-body forces correspond to the Feynman diagram shown in figure 1. Here, we will only briefly look at the expressions for the three-body forces; details can be found in papers [11] and [10]. The Low-Energy-Constants (LEC) parameters used are summarized in the table 1. A cut-off is also introduced as

$$f(\boldsymbol{a},\boldsymbol{b}) = \exp\left\{(\boldsymbol{a}^2+\frac{3}{4}\boldsymbol{b}^2)^2/\Lambda^4\right\} \tag{4}$$

Table 1: Low Energy Constants (LEC). These LECs here are not directly linked to the order NNLO of the chiral effective field theory. See the main text for details in Sec 5.

LEC (Unit)	$3b_0 + b_D$	$2b_2 + 3b_4$ (GeV^{-1})	D'_1	D'_2 ($\mathrm{fm}^2\mathrm{MeV}^{-1}$)	C'_1 (MeV^{-5})	C'_2	C'_3 (MeV^{-5})
[10]	0	−3.0	0	3.628×10^{-3}	4.573×10^{-11}	0	4.573×10^{-11}

where $\boldsymbol{a}$ and $\boldsymbol{b}$ are the Jacobi momenta $\boldsymbol{p}_1 \equiv \frac{\boldsymbol{k}_2 - \boldsymbol{k}_3}{2}$ (or $\boldsymbol{p}'_1$) and $\boldsymbol{q}_1 \equiv \boldsymbol{k}_1$ (or $\boldsymbol{q}'_1$) in the three-body center mass system, respectively. The three-body force also depends on the cutoff parameter, but the expected energy value of the three-body force is at most about 0.1 MeV, and the calculation requires a lot of CPU time, so we provisionally fixed Λ in Eq. (4) to 550 MeV.

The three-body forces used are sandwiched by this cut-off function.

$$V_{3BF}^{YNN}(\boldsymbol{p}_1, \boldsymbol{q}_1; \boldsymbol{p}'_1, \boldsymbol{q}'_1) = f(\boldsymbol{p}_1, \boldsymbol{q}_1)\,\{2\pi \text{ exchange term} + 1\pi \text{ exchange term} + \text{contact term}\} \times f(\boldsymbol{p}'_1, \boldsymbol{q}'_1). \tag{5}$$

3. Binding Energy of Hypertriton

The binding energy B_Λ of the hypertritons from the deuteron threshold has been measured as $102 \pm 63(stat) \pm 67(syst)$ keV[15]. Although we have already published the results of calculations of the binding energy of the hypertriton using traditional meson theory potentials and chiral effective field theory potentials in [12][13], tables 2 and 3 summarize the results (binding energy from the deuteron threshold) of variously changing the order of the chiral potential and the upper limit Λ_c of the cutoff momentum. In [13], only the energy spectrum figure for the cases of NLO13 (Λ_c = 550 MeV) and NLO19 (Λ_c = 550 MeV) is presented. In this work, we aim to explore in detail the dependence of the YN potential on Λ_c. Therefore, Figure 2 shows the spectra in the cases of NLO19 for Λ_c values of 550, 600, and 650 MeV. In addition, a graph of the cutoff dependence of the NN potential is shown in Figure3. First, along the x-axis, we lined up the calculated values including no 3BF (YN), then including 2π exchange type 3BF (YN+2π), then including 1π exchange type 3BF (YN+2π+1π), and finally including contact type 3BF (YN+2π+1π+cnt.).

From both figures, we can see that the 3BFs of the 2π and 1π types are attractive, and the contact type of 3BF is weekly repulsive. The results are stable with almost no change in the cutoff choice Λ_c, but when comparing the cutoff dependency between NN and YN, YN gives more stable results.

4. Kinetic expectation values

The expectation values of the kinetic energy (K_1 and K_2) are calculated from the wave functions Ψ obtained.

$$K_1 \equiv \langle\Psi| \frac{\hat{\boldsymbol{p}}_1^2}{m} |\Psi\rangle = \int\int \Psi^2(\boldsymbol{p}_1, \boldsymbol{q}_1) \frac{\boldsymbol{p}_1^2}{m} d\boldsymbol{p}_1 d\boldsymbol{q}_1,$$
$$K_2 \equiv \langle\Psi| \frac{\hat{\boldsymbol{q}}_1^2}{2\mu} |\Psi\rangle = \int\int \Psi^2(\boldsymbol{p}_1, \boldsymbol{q}_1) \frac{\boldsymbol{q}_1^2}{2\mu} d\boldsymbol{p}_1 d\boldsymbol{q}_1, \tag{6}$$

Table 2: Separation energies of Λ particle in unit keV. The threshold is set at the deuteron and free Λ particle. Not only 2π exchange 3body force but also 1π exchange one are included in the Faddeev calculation. The number inside of the brackets () is the cutoff parameter Λ_c of YN and NN (denoted N^nLO[7]) chiral potential. The unit of Λ_c is MeV.

	YN potential (Λ_c)				
NN potential (Λ_c)	NLO13 [8] (550)	NLO19 [9] (550)	NLO19 (600)	NLO19 (650)	NSC89 [3]
CDBonn [16]	172	194	196	196	317
Nijmegen 93 [2]	114	183	187	191	313
Nijmegen I [2]	120	191	194	196	315
N^4LO+[7] (550)	175	200	204	205	307
N^4LO+ (500)	180	202	205	206	299
N^4LO+ (450)	183	201	204	203	283
N^4LO+ (400)	182	196	197	196	259
N^4LO (550)	178	201	206	208	309
N^4LO (500)	182	203	207	208	300
N^4LO (450)	184	202	205	205	283
N^4LO (400)	183	196	198	197	259
N^3LO (550)	175	200	204	204	300
N^3LO (500)	180	201	205	206	298
N^3LO (450)	184	202	205	205	284
N^3LO (400)	182	196	198	197	261
N^2LO (550)	167	195	205	210	330
N^2LO (500)	183	207	214	216	318
N^2LO (450)	187	206	210	210	292
N^2LO (400)	182	195	197	194	257

where $\boldsymbol{p}_1$ and $\boldsymbol{q}_1$ are Jacobi momenta as used in Eq. (5) and m and μ are nucleon mass (m_N) and the reduced mass ($\frac{2m_N m_\Lambda}{2m_N+m_\Lambda}$) between NN and Λ. m_Λ is the mass of the Λ particle.

Table 4 shows the expectation values of the kinetic energy. First, for the kinetic energy of the deuteron, the calculation values from the conventional meson-theoretic potential (NN: Nijmegen 93 model [2], YN: NSC89 [3]) are compared with the results from the chiral effective field theoretical potentials {NN: N^4LO+ (Λ_c = 550MeV) [7], YN: NLO19(Λ_c = 550MeV)[9])}. The reason why the expectation value of the kinetic energy of the chiral effective field potential is smaller than the traditional one, is thought to be because the function space is restricted by the cutoff. Similar results have been shown for the cases of hypertritons without three-body forces in the third and eighth columns.

As we add 2π, 1π, and cont. type 3BFs in the fourth, fifth, and sixth columns, the effect of each is similar to how they contribute to the bond energy: for the attractive 2π and 1π three-body forces, the expectation value increases, and when repulsive contact type three-body forces are added, the expectation value decreases. We can also see that the contributions from the particle channels of ΣNN (the values in parentheses in the table) show a similar trend.

Table 3: In addition with table 2, the calculation includes not only 2π and 1π exchange 3body forces but also contact type of 3body force.

NN potential (Λ_c)	YN potential (Λ_c) NLO13 [8] (550)	NLO19 [9] (550)	NLO19 (600)	NLO19 (650)	NSC89 [3]
CDBonn [16]	163	185	187	187	300
Nijmegen 93 [2]	148	176	180	183	296
Nijmegen I [2]	154	183	186	187	298
N^4LO+ [7] (550)	166	191	195	196	289
N^4LO+ (500)	170	192	196	196	280
N^4LO+ (450)	173	191	194	193	263
N^4LO+ (400)	171	185	187	184	238
N^4LO (550)	169	192	197	206	290
N^4LO (500)	172	193	197	198	280
N^4LO (450)	174	192	195	194	263
N^4LO (400)	172	185	187	185	239
N^3LO (550)	166	191	195	195	281
N^3LO (500)	171	192	195	196	279
N^3LO (450)	173	191	194	194	264
N^3LO (400)	172	186	187	185	241
N^2LO (550)	188	188	198	203	314
N^2LO (500)	198	198	207	207	300
N^2LO (450)	195	195	200	199	271
N^2LO (400)	184	184	186	182	236

Table 4: Expectation values of the kinetic energy in the hypertriton. There are two types of kinetic energy, K_1 and K_2. K_1 is the kinetic energy related to the first Jacobi momentum of two nucleons, and K_2 is the kinetic energy related to the Jacobi momentum between two nucleons and the Λ particle. The second and seventh columns give the kinetic energy within the deuteron, which is due to the NN potential of N^4LO+ and the Nijmegen model 93, respectively. By adding the YN potential, the third and eighth columns give the kinetic energy of the hypertriton. The fourth, fifth, and sixth columns are the cases when the three forces of 2π, $2\pi + 1\pi$, and $2\pi + 1\pi$ + cnt. are added in sequence, respectively. Also, the numbers in parentheses are not the expectation values for the Λ particle, but the expectation values for the Σ particle instead. Unit is MeV.

Confi-guration	deuteron N^4LO+	N^4LO+ NLO19 no 3bf	N^4LO+ NLO19 2π	N^4LO+ NLO19 $2\pi+ 1\pi$	N^4LO+ NLO19 $2\pi + 1\pi + cnt.$	deuteron Nijm. 93	Nijm. 93 NSC89 no 3bf
N-N: K_1	15.98	16.46	16.85	17.13	16.90	19.30	20.27
Σ	-	(0.12)	(0.17)	(0.20)	(0.19)	-	(0.23)
(NN)-Y: K_2	-	1.87	2.50	2.87	2.81	-	2.20
Σ	-	(0.40)	(0.72)	(0.65)	(0.63)	-	(0.80)
Total	15.98	18.85	20.24	20.75	20.54	19.30	23.51

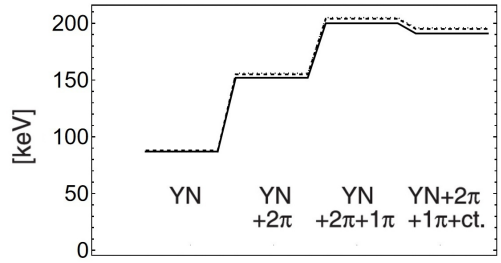

Figure 2: Λ separation energy obtained by Faddeev calculations. Results entries the 2π-exchange, 1π-exchange, and contact 3BFs are added consecutively. The NN interaction is commonly the semilocal N^4LO^+ interactions [7] with a cutoff of 550MeV. There are solid, dashed, dotted lines that correspond to the YN's NLO19[9] cutoff scale Λ_c of 550 MeV, 600 MeV, and 650 MeV, respectively.

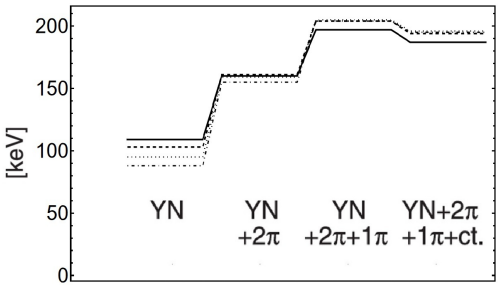

Figure 3: Similar to figure 2, but the common NN interactions are the semilocal N^4LO^+ interactions [7]. There are solid, dashed, dotted and dash-dotted lines that correspond to the NN cutoff scale Λ_c of 400, 450, 500 and 550 MeV, respectively. The cutoff scale Λ_c of the chiral YN interactions (NLO19) [9] is commonly used 600 MeV.

5. Conclusion and Outlook

The YNN three-baryon system is simply a case of replacing one nucleon in a three-nucleon system with a hyperon. However, determining the parameters contained in the basic interacting YN potential is a challenging task, particularly in two-body scattering experiments, and it is even more difficult to infer the three-body force. The chiral effective field theory has a prescription that enables the consistent introduction of not only three-body forces but also many-body forces of more than three bodies. A notable advantage of this approach is the ability to determine three-body forces by increasing the chiral order.

However, the chiral order appears to be somewhat contradictory, as starting from the NNLO order, three-body forces emerge. Therefore, given that the YN potential NLO19 with which we are working is literally NLO, it may be premature to discuss three-body forces. The low-energy constants for three-body forces that we used are those described in [10] and are based on an isobar saturation model. Recently, NNLO-order papers [17, 18] on YN potential were published. These papers allow for the calculation for the parameters $(3b_0+b_D)$ and $(2b_2+3b_4)$ in Table 1, resulting[2] in -1.485 and -3.01 GeV $^{-1}$, respectively. The value for $(2b_2+3b_4)$ is approximately consistent with the NNLO value, but for $(3b_0+b_D)$, it was simply ignored at this stage. In the future, the accumulated analyses of high-precision experiments such as [5, 19–22] will further improve the accuracy of 1π exchange and contact-type three-body force parameters (C_n' and D_n').

Acknowledgements. This work is supported by JSPS KAKENHI Grants No. JP19K03849, No. JP22K03597, No. JP24K07019, and JP25K07301.

[2]The b_0, b_D, b_2, and b_4 used are taken from [17], i.e., b_D=0.066, b_0=–0.517[23], b_2=0.76, b_4=–1.51 GeV^{-1}.

References

[1] K. Miyagawa, H. Kamada, W. Glöckle, and V. Stoks, Phys. Rev. C **51**, 2905 (1995).

[2] V. G. J. Stoks, R. A. M. Klomp, M. C. M. Rentmeester, J. J. de Swart, Phys. Rev. C **48**, 792 (1993).

[3] P. M. M. Maessen, Th. A. Rijken, J. J. de Swart, Phys. Rev. C **40**, 2226 (1989).

[4] H. Kamada, J. Golak, K. Miyagawa, H. Witała, W. Glöckle, Phys. Rev. C **57**, 1595 (1998) .

[5] S. Acharya *et al.* (ALICE Collaboration), Phys. Rev. Lett. **131**, 102302 (2023).

[6] E. Epelbaum, W. Glöckle, Ulf-G. Meißner, Nucl. Phys. A **747**, 362 (2005).

[7] P. Reinert, H. Krebs and E. Epelbaum, Eur. Phys. J. A **54**, 86 (2018).

[8] J. Haidenbauer, S. Petschauer, N. Kaiser, U.-G. Meißner, A. Nogga, and W. Weise, Nucl. Phys. **A915**, 24 (2013).

[9] J. Haidenbauer, U.-G. Meißner and A. Nogga, Eur. Phys. J. A **56**, 91 (2020).

[10] S. Petschauer, N. Kaiser, J. Haidenbauer, U.-G. Meißner and W. Weise, Phys. Rev. C **93**, 014001 (2016).

[11] M. Kohno, H. Kamada and K. Miyagawa, Phys. Rev. C **106**, 054004 (2022); [Erratum: Phys. Rev. C **110**, 019906(E) (2024)].

[12] H. Kamada, M. Kohno and K. Miyagawa, Phys. Rev. C **108**, 024004 (2023); [Erratum: Phys. Rev. C **110**, 019907 (2024)].

[13] M. Kohno, H. Kamada and K. Miyagawa, Phys. Rev. C **109**, 024003 (2024); [Erratum: Phys. Rev. C **110**, 019908 (2024)].

[14] H. Le, J. Haidenbauer, H. Kamada, M. Kohno, U.-G. Meißner, K. Miyagawa, Eur. Phys. J. A **61**, 21 (2025), https://arxiv.org/abs/2407.02064 (2024).

[15] S. Acharya *et al.*, Phys. Rev. Lett. 131, 102302 (2023).

[16] R. Machleidt, Phys. Rev. C **63**, 024001 (2001).

[17] J. Haidenbauer, U-G. Meißner, A. Nogga, H. Le, Eur. Phys. J. A**59**, 63 (2023).

[18] H. Le, J. Haidenbauer, U.-G. Meißner, and A. Nogga, Eur. Phys. J. A**60**, 3 (2024).

[19] J. Rowley *et al.*, Phys. Rev. Lett. **127**, 272303 (2021).

[20] K. Miwa *et al.*, Phys. Rev. C **104**, 045204 (2021).

[21] K. Miwa *et al.*, Phy. Rev. Lett. **128** , 072501 (2022).

[22] T. Nakamura *et al.*, PTEP **2022** 093D01, (2022).

[23] V. Bernerd, N. Kaiser, U.-G. Meißner, Int. J. Mod. E **4**, 193 (1955).